



Türkenschanzstrasse 17, A-1180 Wien

Bachelor Thesis

Statistical Significance of the Bimodality in Chromospheric Activity

Tobias Sutter (01507794)
Field of Study: Astronomy (A 033 661)

Supervisor: Sudeshna Boro Saikia
To be handed in until: 30.09.2018

Abstract

Due to the constantly growing amount and accuracy of available chromospheric activity data for F- to M-stars, the existence of the Vaughan-Preston-Gap and therefore the non-existence of intermediate-activity stars, have been questioned. The existence of the gap has never been tested statistically with the new data, thus, accomplishing this task with 3064 sample stars is the main focus of this work. To be able to identify the significance of the Vaughan-Preston-Gap, the Dip-test of Unimodality by Hartigan and Hartigan (1985) is used to determine the probability of the distribution to be unimodal. Furthermore, a normal distribution was fitted to the data to observe the correlation of the data to this unimodal distribution. For F- and G-stars in the range of $0.44 < B-V < 1.1$, where the Vaughan-Preston-Gap was originally defined, the data shows strong unimodality with a P-value of 0.88. Going to K-stars with $1.1 < B-V < 1.4$, this unimodality appears to get even stronger with a P-value of 0.98. Only very late M-stars with $1.4 < B-V < 2.0$ show some sort of bimodality with a P-value of 0.4. Based on the findings for F- and G-stars, we conclude that there is no gap in activity as suggested by Vaughan and Preston (1980). This result is backed up by rotational data. Hence, theories of rapid spindown and different dynamo mechanisms are most likely not correct.

Contents

1	Introduction and Motivation	1
1.1	What is a chromosphere?	2
1.2	What stars have chromospheres?	2
1.3	Chromospheric Activity	2
1.3.1	What is chromospheric activity?	2
1.3.2	Observations and surveys of CaII H & K	4
1.3.3	The flux index S and the index R'_{HK}	4
1.4	The Vaughan-Preston-Gap	5
2	Methods/Data analysis	7
2.1	The Vaughan-Preston-Gap and Bimodality	7
2.2	The new dataset	8
2.3	Uni- vs. Bimodality	8
2.4	Statistical test of Unimodality	9
2.4.1	Hartigan's Dip test	9
3	Results	11
3.1	The original Mt. Wilson dataset (Noyes et al. 1984)	11
3.2	The new dataset	11
3.3	The three subsets	13
3.3.1	Subset 1: $0.44 < B-V < 1.1$	13
3.3.2	Subset 2: $1.1 < B-V < 1.4$	14
3.3.3	Subset 3: $1.4 < B-V < 2.0$	15
3.4	Observational evidence of the nonexistence of the VP-Gap	16
4	Discussion and Conclusion	19

1 Introduction and Motivation

Since the first discovery of a rocky exoplanet, researchers always wanted to know, whether it is habitable or not. If a planet can sustain life depends on four fundamental parts. Those are complex molecular chains, nutrients, liquid water and a supply of energy. For water to be liquid, both the surface pressure and temperature have to be right. Neglecting the pressure for now, the temperature mainly depends on the chemical composition of the atmosphere and the radiated energy from the central star, which, in return, is highly dependent on the activity of the host star. So if we understand the processes which lead to active stars, we are also one step closer to understand the habitability of exoplanets.

The chromospheres of our sun and stars like it remain a big mystery up until today. This mysteriousness stems from the fact that we still have not fully understood the temperature rise in this layer of our own central star and the complex physical processes involved in it. This heating mechanisms are generally called activity and can very well be observed in many far away stars with today's technical means. Almost half a century ago, the observed sample was not as big as it is today. Probably as a result of that, Vaughan and Preston (1980) found in their survey of Field Stars in the solar neighborhood that there is a gap in activity. Based on this work and seeing that there are high activity stars and low activity stars, but none in between, Noyes et al. (1984) concluded, that there are three main possibilities for why the gap exists.

The first one they proposed was, that the gap is not real and just a statistical remnant of the chosen stars in the solar neighborhood.

Secondly, they suggested, that the gap is statistically significant even though the rotation rate and chromospheric activity decrease smoothly, but in the solar neighborhood are no stars with mediocre activity. Therefore, the gap only describes the lack of medium chromospheric activity levels of stars in the solar neighborhood.

And the last attempt to explain the gap was that there must be a rapid spindown from high activity/high rotation stars to low activity stars with a low rotation rate. Because this spindown happens so fast, the probability for us to see a star with medium activity is very low. The rapid spindown also implies, that two different dynamo processes may be existent in a stars lifetime.

All this happened more than three decades ago and nowadays it is widely believed, that the gap is only a statistical remnant of the early work on this topic. Although it is mostly accepted across the community, this possible bimodality in chromospheric activity has to be tested to be absolutely sure.

To answer this question would also be a big help in finding possible candidates for habitable planets because the temperature of the atmosphere on exoplanets and thus the range of the habitable zone mainly depends on the radiated energy of the central star, which is directly linked to the chromospheric activity. So if we understand the chromospheric activity of stars, we are more likely to be able to predict, which potential exoplanet could be habitable and which could not.

Furthermore, since the relation of the rotation rate and the chromospheric activity is not fully understood so far, this is also a topic to investigate.

1.1 What is a chromosphere?

Above the stellar photosphere, the region of a star from which the majority of its light is radiated, and below the corona, lies the chromosphere. The chromosphere is a heterogenous layer of the stellar atmosphere. Its temperature and density profiles are very different from the stellar photosphere. The heterogenous nature of the solar chromosphere is shown in Figure 1.

Observations of the solar atmosphere have shown, that there is a sudden rise in temperature as one moves away from the photosphere towards the chromosphere and the corona. This does not correspond to the expectations when we assume radiative equilibrium. After the temperature falls all the way from the core to the outermost part of the photosphere, it starts to slowly rise up to about 7000 K in the chromosphere and rises more abruptly higher in the atmosphere. The rapid temperature rise occurs in an area of the stellar atmosphere known as the transition region. Finally, the temperature is hottest at the corona reaching up to a million Kelvin (see Hall et al. 2008 for more details).

The heating of the upper layers of the stellar atmosphere is non-thermal in nature and is caused by the stellar magnetic field and activity (see Chapter 1.3 for more details).

This magnetic heating of the chromosphere can be observed in the form of emission in certain resonance and Balmer lines. Examples for this are the CaII- or MgII-lines.

1.2 What stars have chromospheres?

Chromospheres are primarily present in sun-like dwarfs (spectral type F to M). Thick chromospheres are expected to be found in cool stars. This is based on the fact that their plasma can still be ionized by the additional mechanical heating processes above the photosphere. Hot stars do not have enough non-ionized hydrogen left on their surfaces to support extended chromospheres found in cool stars. However, some hot stars are known to exhibit weak chromospheres. For more detail, see Linsky (2017).

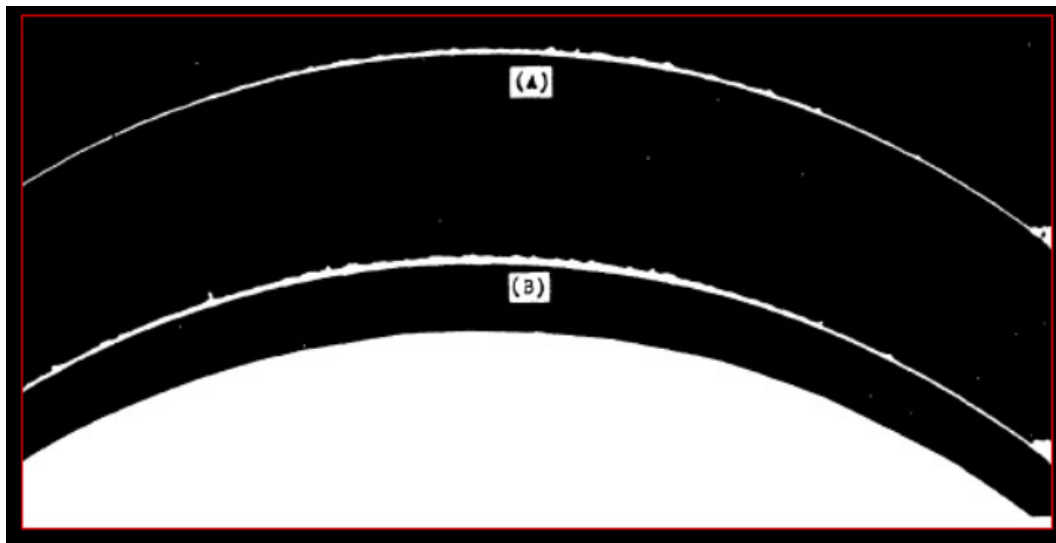


Figure 1: Image (A and B) showing the chromosphere of the Sun (Roberts 1945). The pictures were taken eight minutes apart. It clearly shows the heterogenous, quickly fluctuating nature of chromospheres.

1.3 Chromospheric Activity

1.3.1 What is chromospheric activity?

As mentioned earlier, the chromosphere does not follow radiative equilibrium. In theory, under radiative equilibrium, the energy in a stellar atmosphere is solely transported by radiation through the plasma. When the plasma absorbs part of this radiation, it gives it back to the total photon flux via thermal emission. This ensures the outward flow of energy from the star's core into space. However, observations of emission reversal

in solar and stellar Fraunhofer lines (396.847 and 393.368 nm respectively) indicates deviation from radiative equilibrium. Linsky (2017) offers a more detailed insight in this topic.

Under normal circumstance, these lines are absorption features, so this extra emission should not be present. Consequently, there must be an additional heating mechanism that explains these radiative losses. The heating mechanism is called activity and can be divided into two distinct forms. The first and probably the biggest of those two has to do with stellar magnetic fields. They heat the chromosphere as well as the corona by dumping mechanical energy in those layers, transported along magnetic “conduits” (see Hall et al. 2008 for more details). Additionally, as stellar magnetic fields are assumed to be mostly created by the convection zone of a star, we will find extended chromospheres usually in stars where such convective mechanisms are present. These phenomena are an important property of late A and cooler stars. Alternatively, another possibility was proposed by Biermann (1948) and Schwarzschild (1948), in which the additional heating of the chromosphere was due to a continuous stream of acoustic waves. These waves would eventually evolve into shocks and dissipate in the outer layers of a star, therefore feeding the chromosphere with additional energy and heating it.

While getting heated up by those effects, the hydrogen in the plasma gets ionized. The now free electrons allow collisional radiative cooling and thus create additional emission. One of the most well known examples are the CaII H & K emission lines, shown in Figure 2.

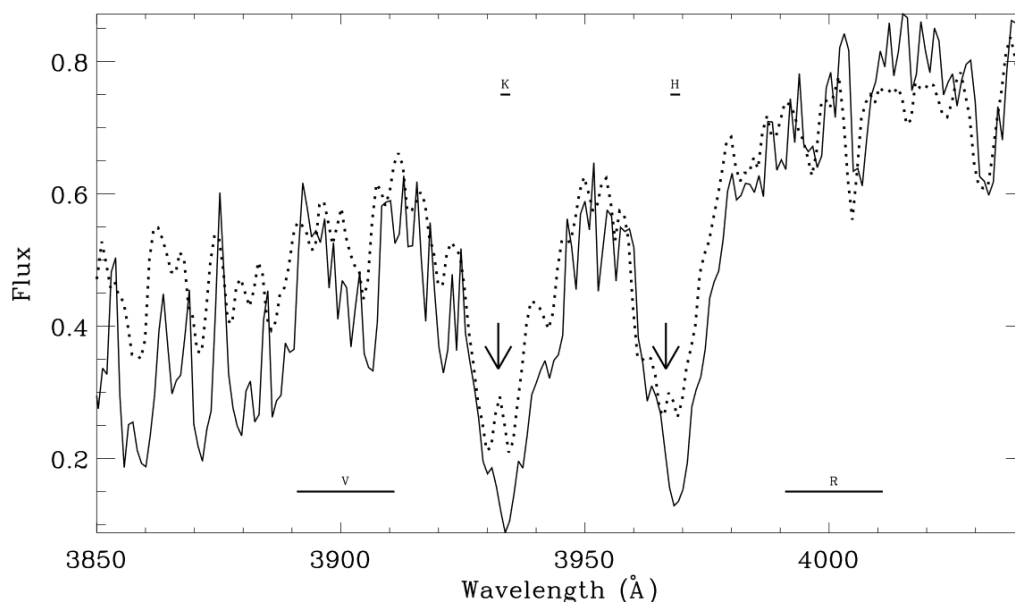


Figure 2: A spectrum of an inactive (solid line) and one of an active (dotted line) star. The emission reversal for the active star in the CaII H & K lines can be seen very easily and is pointed out by the two arrows. The pseudo-continuum reference bandpasses V & R can be seen on either side of the absorption lines. This figure is taken from Fig. 3 of Zhao et al., 2013, *The Astronomical Journal*, 145.

1.3.2 Observations and surveys of CaII H & K

Since the first detection of CaII H & K emission lines in stellar spectra by Eberhard & Schwarzschild (1913), these two resonance lines have become synonymous with chromospheric activity.

One of the primary source of stellar chromospheric data is the HK project, carried out at the Mount Wilson Observatory in California. This project lasted from 1966 until it was stopped in 2003. The first observations were made by Wilson (1978), followed by the observation of a few hundred stars by Vaughan and Preston (1980), where they identified the gap in activity, also known as Vaughan-Preston-Gap. Duncan et al. (1991) went one step further and observed 1296 stars. After that, Baliunas et al. (1995) made a long-term time series of observations. They were able to show, that cool stars can have sun-like activity cycles. Additionally, they can also have irregular but highly variable activity or Maunder minimum-like states. Baliunas and Soon (1995) showed, that the mean level and the amplitude of chromospheric variability is related to the length of the chromospheric activity cycle. This means the longer the cycle, the smaller the amplitude/mean activity level and vice versa. Three years later, again a study by Baliunas et al. (1998) showed that 60% of the observed stars showed periodic, cyclic variations. Only 25% showed irregular or non-periodic variability and 15% showed little to none activity.

Since the Mount Wilson project, multiple other long term surveys of chromospheric activity have been carried out, for example by Arriegada (2011), Mittag et al. (2013), Isaacson & Fischer (2010), Hall et al. (2009) and Mamajek & Hillenbrand (2008).

1.3.3 The flux index S and the index R'_{HK}

In order to determine the chromospheric activity correctly, we need a suitable parameter. Since chromospheric activity is linked to the emission reversal in the CaII H & K lines, it can be used to define an index of activity. Duncan et al. (1991) defined an instrumental index "S" to measure the activity from CaII H & K lines

$$S = \alpha \cdot \frac{N_H + N_K}{N_R + N_V} \quad (1)$$

where α is a constant of proportionality and is determined empirically. In their original survey, Duncan et al. (1991) determined the variation of α to be less than the actual measurement accuracy and thus it was set to $\alpha = 2.40$.

The index S is the ratio of the sum of the emission in the H and in the K band (at 396.847 nm and 393.368 nm respectively, FWHM = 0.1 nm), compared to the emission in the 2 nm-wide pseudo-continuum bands R (399.107 nm-401.107 nm) and V (389.107 nm-391.107 nm), which lie on either side of the emission lines. If the emission in the H and K bands is very high, the S-index will be rather high as well, because the pseudo-continuum should stay the same. Hence, the S-index reflects the chromospheric activity of a star.

Although the S-Index is far from the optimal index describing activity, it is a very good approach and its predominant usage in the analyses of the HK Project data makes us use it up until today. The problem with this index is, however, that we cannot directly compare the S values of two stars with different spectral type because these objects have different temperatures and thus the flux in the pseudo continuum is different. The S-Index is still a good approximation, but this problem needs to be addressed.

To calibrate the S values to absolute flux, based on the work of Middelkoop (1982), Rutten (1984) introduced a color-dependent factor which relates continuum counts in the pseudo-continuum bandpasses R & V between stars of different temperature. It is called C_{cf} and defined as follows,

$$F_H + F_K = SC_{cf}T_{eff}^4 10^{-14} \quad (2)$$

$$\log C_{cf} = 0.24 + 0.43(B - V) - 1.33(B - V)^2 + 0.25(B - V)^3 \quad (3)$$

If this is normalized by the bolometric flux ($T_{eff}^4 10^{-14}$), we get a new value

$$R_{HK} = SC_{cf} = \frac{F_H + F_K}{T_{eff}^4 10^{-14}} \quad (4)$$

This flux value is now corrected for the variations with temperature. Noyes et al. (1984) suggested, that if the emission of the photosphere is subtracted from that value, the result would be the true chromospheric emission ratio

$$R'_{HK} = R_{HK} - R_{phot} \quad (5)$$

This is the purely chromospheric fraction of the flux in the CAII H&K bands. The photospheric flux is calculated by the cubic equation

$$\log R_{phot} = -4.898 + 1.918(B - V)^2 - 2.893(B - V)^3 \quad (6)$$

Note, that this formula only depends on B-V and not on chromospheric activity. This is not strictly true for all stars according to White and Livingston (1981), but accurate enough for this work.

Since activity is examined over the spectral range of F-M, in this work, the R'_{HK} -Index will be used.

1.4 The Vaughan-Preston-Gap

Back in 1980 Arthur H. Vaughan and George W. Preston took a look at 396 field stars in the solar neighborhood observed by the Mount Wilson project. Their aim was to provide a (for their time) big sample of chromospheric activity exhibited by field stars. The sample was meant to be unbiased with respect to age.

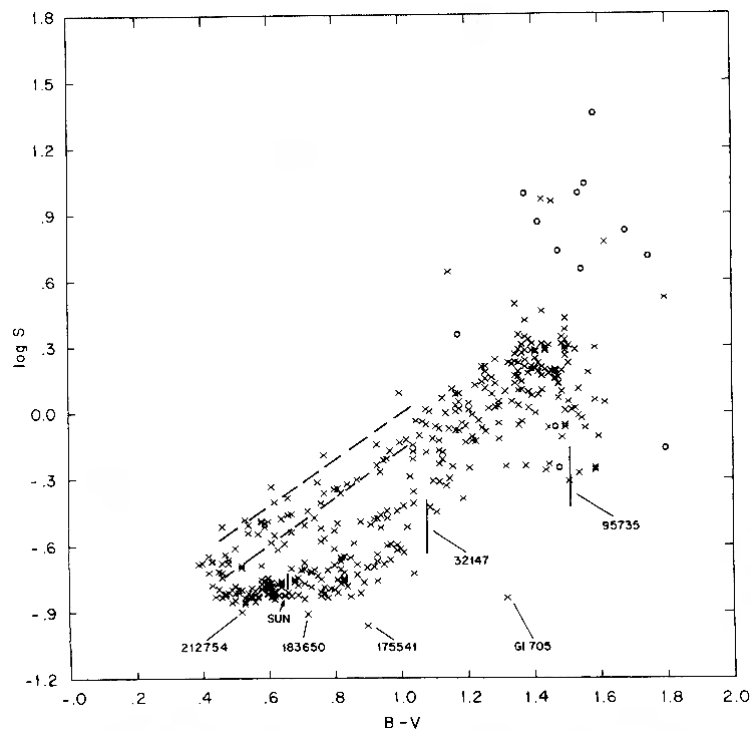


Figure 3: Chromospheric activity ($\log S$) vs. B-V color. On the x-axis is the color/temperature of 396 field stars in the solar neighborhood, the y-axis represents the (logarithmic) activity of these stars. This figure is taken from Fig. 1 of Vaughan and Preston, 1980, Publ. Astron. Soc. Pac., 92.

Figure 3 shows the chromospheric activity as a function of B-V, taken from Vaughan and Preston (1980). The authors divided the stars into four distinct groups.

Group I is the smallest of the four and consists of mostly dMe stars. It is in the upper right corner of the diagram. The second group contains stars of $1.1 < B-V < 1.6$, which are mainly late K and M stars. Almost the entirety of those stars show strong CaII emission. Groups III and IV consist of F- & G-stars ($0.44 < B-V < 1.1$). There appears to be a lack of stars between these two groups, resulting in an apparent gap. This gap defines the boundaries of group III with the very active stars and high HK emission and group IV, consisting of stars with low activity showing only weak HK emission. The Sun only shows little activity and is thus on the bottom half of the gap. There seem to be no intermediate activity stars. This apparent activity gap is called Vaughan-Preston-Gap, referred to as the VP-Gap from here on.

Vaughan and Preston (1980) provide two possible explanations for the existence of the gap. Firstly, they state that the gap could be present because of an abrupt drop in chromospheric activity at an age of around one Gyr. The second possibility could be, that their sample was not big enough and thus the gap is a unique characteristic of the 396 stars in their sample.

They recommended, that further investigation with an increased sample is required to address this question. An independent study of the VP-Gap was also carried out by Noyes et al. (1984), using data from the long-term survey of Wilson (1978). Although this sample is significantly smaller, it is largely independent. Firstly, they recreated the plot of Vaughan and Preston with $0.44 < B-V < 1.1$. Their results agree with the results of Vaughan and Preston (1980). To account for different spectral types, they calculated the R'_{HK} from the S values for these stars. Figure 4 shows the $\log R'_{HK}$ vs. B-V taken from Noyes et al. (1984). With this color-correction, the “slope” of the gap is not as steep. Nevertheless, the VP-Gap between $0.44 < B-V < 1.1$ is still present. Closed and open circles represent “young” and “old” stars respectively. This classification was done by Vaughan (1980) based on activity cycles. Figure 4 shows, that the VP-Gap furthermore separates the stars based on age, with young stars being on the top half and old stars being on the bottom half.

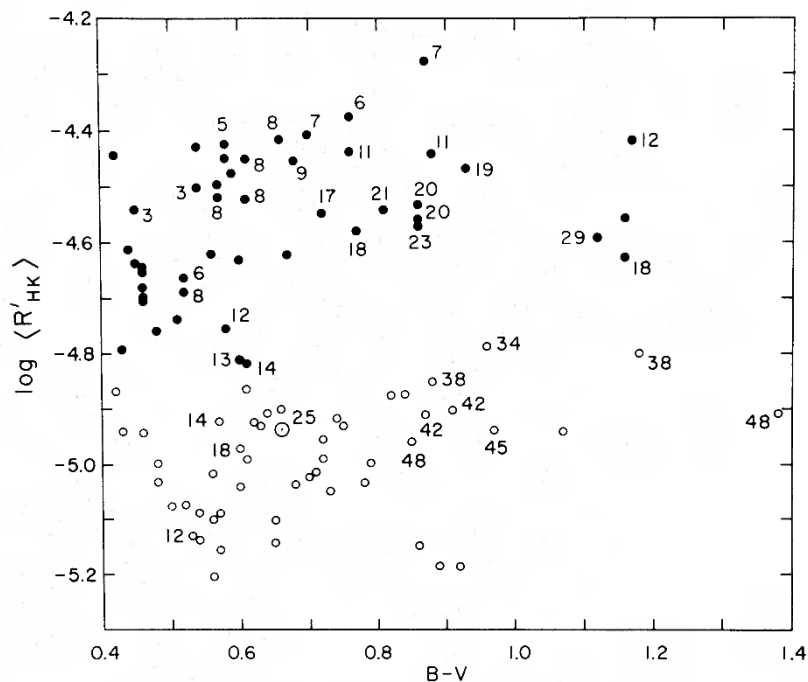


Figure 4: $\log R'_{HK}$ vs. B-V. The Sun is represented by \odot . Closed and open circles represent “young” and “old” stars respectively. The labels are the rotation periods of the stars rounded to the nearest day. Taken from Fig. 2 of Noyes et al. 1984, *Astrophys. J.*, 279.

2 Methods/Data analysis

2.1 The Vaughan-Preston-Gap and Bimodality

In Figure 5, the histogram of the data used by Noyes et al. (1984) is shown. To generate this plot, the values are projected on the y-axis and counted. The histogram is normalized, where the area under the histogram adds up to 1. This task is achieved by dividing the count by the number of observations times the bin width instead of dividing by the total number of observations. Thus, the unit of the y-axis is dimensionless. This will be alike in all the following histograms. As can be clearly seen in this figure, there seem to be two different peaks of the distribution function at around -4.5 and -5.0 respectively, which would imply a bimodal distribution. The dotted red lines show the estimated boundaries of the VP-Gap, the solid line is the center of the VP-Gap. This illustrates nicely again, that for Noyes et al. (1984), the gap was pretty evident.

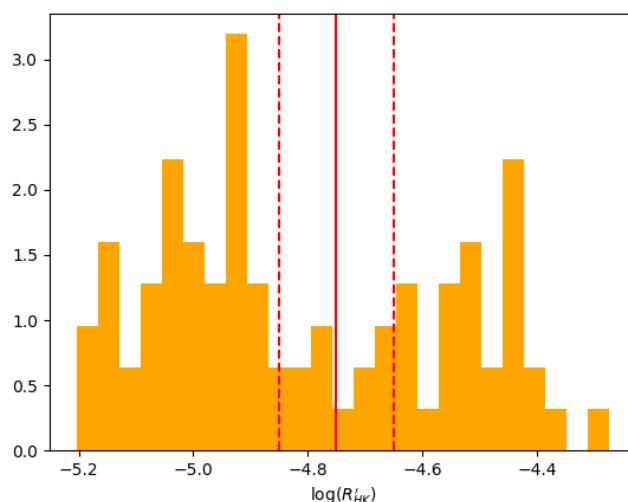


Figure 5: The histogram of the data used by Noyes et al. (1984). It is normalized, thus the units of the y-axis are dimensionless. The bimodality can be seen quite nicely, with center peaks of the distribution at around -4.5 and -5.0. The dotted red line signifies the boundaries and the solid line is the center of the VP-Gap.

In the rather small sample Vaughan and Preston (1980) or Noyes et al. (1984) used, as shown in Fig. 5, the Vaughan-Preston gap indicates a bimodality in chromospheric activity. Noyes et al. (1984) provides three different explanations supporting the existence of the gap. The first one is, that the gap is simply the result of the random selection of the stars in a rather small sample. If so, when we increase our sample size, the gap should disappear and the stars should be distributed smoothly. The second explanation they provide, is, that the gap is real but only for the solar neighborhood, from which the data was collected. Therefore the age-activity-distribution in our nearest solar surrounding is bimodally distributed. The last possible explanation is, that the gap is in fact present and real for all stars in the universe. They state, that the gap is the result of a rapid spindown process, which happens to stars transitioning from “young” to “old” stars. This would explain the lower R'_{HK} rates. Because this happens relatively fast, there are practically no stars in between the active and inactive branches. It also would mean that stars with $0.4 < B-V < 1.1$ always show bimodality, regardless of the sample size.

Another way of explaining the gap is by considering the stellar dynamo. Durney et al. (1981) suggested, that the gap is the result of the change in the stellar dynamo. Böhm-Vitense (2007) proposed the theory, that the rapid spindown of stars is an indicator that there must be different dynamos active throughout a star’s lifecycle, which would lead to the differences in chromospheric activity that Vaughan and Preston (1980) or Noyes et al. (1984) observed.

If stars are, against the evidence from the sample, indeed unimodally distributed, it would mean, that probably the spindown process would be much more smoothly. This would also eliminate the theory about the changing

dynamo effects in a star throughout its lifetime. The question, whether stars are distributed unimodally or bimodally can probably only be answered by a reasonably big sample size, which we have today. This new data now has to be checked quantitatively for uni-/bimodality.

2.2 The new dataset

The dataset used in this work consists of chromospheric activity data ($\log R'_{\text{HK}}$) and B-V of 3064 stars taken from Boro Saikia et al. (2018). The data on these stars was gathered from Arriagada (2011), Wright et al. (2004), Isaacson & Fischer (2010), Henry et al. (1996), Gray et al. (2006), Hall et al. (2009), Lovis et al. (2011), Bonfils et al. (2013) and Duncan et al. (1991). Fig. 6 shows the $\log R'_{\text{HK}}$ vs. B-V for the entire sample. This plot is essentially the same as Noyes et al. (1984) but with a sample 33 times the size in their work. As shown in Fig. 6, the VP-Gap is not as easily detected as in Noyes et al. (1984). Between $0.44 < \text{B-V} < 1.1$, the gap even seems to disappear. There are some additional features in the plot. Beyond $\text{B-V} > 1.1$, chromospheric activity exhibits different behavior when plotted as a function of B-V. However, the key focus in this work lies on stars with B-V between 0.44 and 1.1.

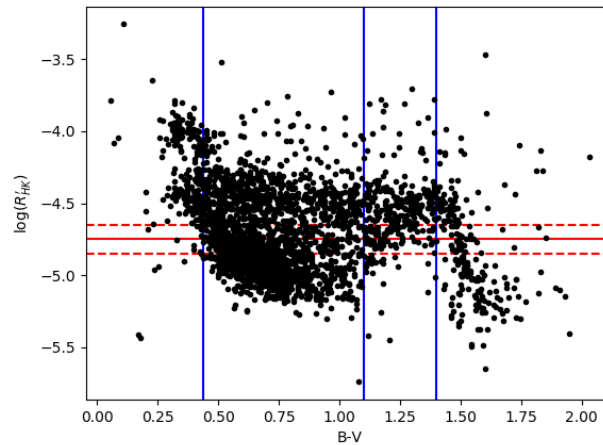


Figure 6: This is basically the same plot as Fig. 4 from Noyes et al. (1984) but only with 3064 data points rather than only 95. The dotted red horizontal lines indicate where the borders of the VP-Gap should be, the solid line represents its center. The VP-Gap is not easily visible anymore. The data was split into three different datasets (blue vertical lines): **1.:** F- and G-stars from $0.44 < \text{B-V} < 1.1$, **2.:** K-stars from $1.1 < \text{B-V} < 1.4$, **3.:** M-stars from $1.4 < \text{B-V} < 2.0$

2.3 Uni- vs. Bimodality

In order to determine the existence of the Vaughan-Preston gap, statistical tests can be performed to determine its uni-/bimodality. A unimodal distribution is a probability distribution that has only one peak, as shown in Fig. 7(a) (blue curve). Around the value of this peak, the remaining data points are scattered. For example, a normal or Poisson distribution is a unimodal distribution. Contrary to a unimodal distribution, a multimodal distribution will have more than one peak. The case where there are exactly two highest values is called bimodal.

To illustrate the two kinds of distributions (unimodal and bimodal), a few simulations were carried out using Python, as shown in Figure 7. For each of the figures, two different distributions are simulated (1000 random sample values each) with different mean values (μ) and standard deviations (σ). μ_1 and σ_1 refer to the left of the red curves, μ_2 and σ_2 refer to the right of the red curves. The randomly distributed data is plotted in normed histograms so they act as a random probability distribution. The subfigures of Figure 7 show both distributions in the same graph. The red curves in the plots show the fit of a normal distribution to either of the two randomly generated 1000 sample values, the blue curve is the sum of the two fits. Thus, the blue one is the overall probability distribution of the whole distribution.

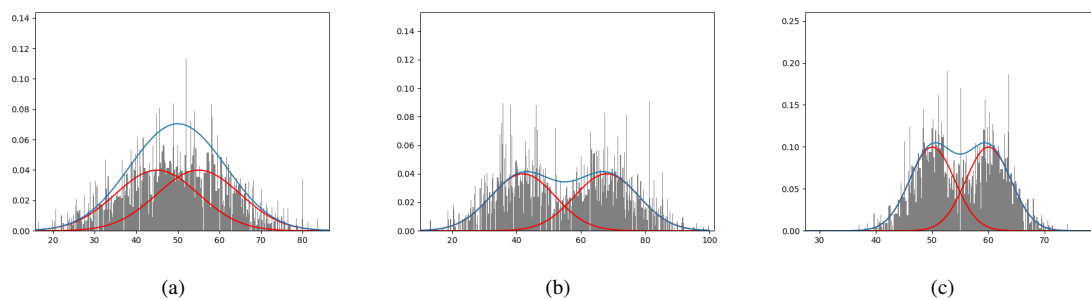


Figure 7: Distributions with different μ_1 , σ_1 , μ_2 , σ_2 values. (a) $\mu_1 = 45$, $\sigma_1 = 10$, $\mu_2 = 55$, $\sigma_2 = 10$. (b) $\mu_1 = 40$, $\sigma_1 = 10$, $\mu_2 = 65$, $\sigma_2 = 10$. (c) $\mu_1 = 50$, $\sigma_1 = 4$, $\mu_2 = 60$, $\sigma_2 = 4$

In Fig. 7(a) we can examine, that even if there are two underlying normal distributions, the overall distribution still can be unimodal. Figure 7(b) stretches the centers of the two individual curves more apart and thus the overall distribution is bimodal. The same is the case in Figure 7(c).

The above example shows the key difference between a unimodal and a bimodal distribution. However, in order to test the uni-/bimodality of a sample, further statistical tests are needed. In this work, the dip test is used to test the uni-/bimodality of the sample described in Section 2.2.

2.4 Statistical test of Unimodality

There are several tests to find out if a dataset is distributed in a unimodal or a bimodal fashion. Graphical methods such as histograms or scatter plots can be used as a first hand estimate to determine the unimodality or bimodality of a dataset. If the distribution tends to be very bimodal, the plot should clearly show two separate branches. This method was used in the work of Vaughan and Preston (1980) and Noyes (1984) to determine the existence of the VP-Gap. Another way of testing the bimodality of a distribution is to check, whether the dataset can be split up into two different unimodal distributions. These are theoretically just overlapping functions and thus creating the whole sample. A statistical test using this method was first proposed by Pearson (1894). This test is optimal, if one wants to show that a dataset is bimodal and find out the underlying distribution functions.

The work of Boro Saikia et al. (2018) suggested, that in light of new data, the VP-Gap is insignificant. However, the authors do not perform any statistical tests to determine the uni-/bimodality of the data. In this work, the multimodality of the data in Boro Saikia et al. (2018) is tested by using the Hartigan's dip test. This test only gives us information about whether a distribution is unimodal or not. If the distribution is not unimodal, it doesn't give us information about the number of modes of the distribution. Since we want to test the unimodality of the data (as suggested by the recent work of Boro Saikia et al. 2018) the dip test is used. It is, however, not the only test available to check unimodality of a dataset. Bandwidth test is another such test and can be used instead.

The diptest of unimodality was first suggested by Hartigan and Hartigan (1985). A Python implementation of the test is used. The Python implementation is based on the existing R package¹ which was implemented by K. Johnsson and made publicly available on Github².

2.4.1 Hartigan's Dip test

The diptest can be explained as follows. Firstly, the frequency distribution is transformed into a cumulative frequency distribution. This does not matter in terms of uni-/bimodality and is only used for easier calculation because now the minimum value is 0 and the maximum value is 1. The best fitting unimodal distribution to the dataset is then determined. This is a mixture of the greatest convex minorant and the least concave majorant for the cumulative distribution. To identify the unimodality of our data, the greatest difference of the fitted distribution to the empirical distribution is calculated. This difference is called the Dip and in combination

¹<https://cran.r-project.org/web/packages/diptest/diptest.pdf>

²<https://github.com/kjohnsson/modality>

with the sample size it is a measure of the unimodality of the distribution. The sample size is important because since we have a discrete rather than a continuous distribution, this gap becomes generally smaller with increasing sample sizes and vice versa. The calculation of the Dip for a discrete distribution is done with an algorithm, which can be found in Hartigan and Hartigan (1985) Section 4.

The relation of the Dip to the unimodality becomes clearer if we take a look at two examples. Firstly, let's suppose we have a totally unimodal distribution of our data with arbitrarily large sample size. Therefore, the discrete distribution approaches a continuous distribution. If we now calculate the best fitting unimodal distribution to the data, we will essentially get back a copy of the data. And if we calculate the biggest difference, we will basically get zero. So we have a small dip for a unimodal distribution.

The other example is one of a completely bimodal distribution, where we have two peaks of different unimodal distributions which are far apart. These two unimodal distributions do not touch each other, which means, that we have a complete gap in between. Again, the sample size is large. If we now calculate the best fitting unimodal distribution to this data, we will get a function, which, at the side slopes, increases like our unimodal distributions and is constant between the two peaks. Thus, the biggest difference of the calculated function and our data is the height of the two peaks. This logically leads to a big dip for a bimodal distribution.

To describe the calculation procedure of the Dip mathematically, we first define

$$\rho(F, G) = \sup_x |F(x) - G(x)| \quad (7)$$

for any bounded functions F, G . This is the maximum distance between those two functions. If we don't work with only one function G but rather with a whole class of bounded functions \mathcal{A} , we can define

$$\rho(F, \mathcal{A}) = \inf_{G \in \mathcal{A}} \rho(F, G) \quad (8)$$

Thus, we get the best fitting function to our initial distribution function F . We can now further restrict our class of functions to \mathcal{U} , which only includes unimodal functions. These are by definition also bounded functions, which means that \mathcal{U} is a subclass of \mathcal{A} . Then, the dip D of our distribution function F is defined by

$$D(F) = \rho(F, \mathcal{U}) \quad (9)$$

As we already found out earlier, if F is unimodal itself, so $F \in \mathcal{U}$, then the dip $D(F) = 0$. This fact let us also conclude that if $F \notin \mathcal{U}$, then the dip $D(F) > 0$. So the dip is a measurement of unimodality. This mathematical structure works for continuous as well as for discrete functions F , even though then the second to last statements is not true anymore. The result of the Dip has to be seen statistically, with better accuracy for bigger sample sizes, rather than with absolute certainty. Therefore a Dip $D(F) = 0$ is not possible with a discrete distribution F with sample size n , but with increasing n the Dip $D(F)$ approximates to 0. In general, this also means that the Dip of a unimodal distribution with small n can be rather big compared to a bimodal one with significantly larger n .

The next step is to quantify the size of the Dip and correlate it to the probability of the distribution being unimodal or not, which is further on referred to as the P-value. To successfully accomplish this, we have to again utilize statistics. The basis of this is the simulation of numerous unimodal distributions with a specific sample size n . Hartigan and Hartigan (1985) did the simulation of 9999 different unimodal distributions for different n . When we do the Diptest for all of these distributions, we can calculate the percentage P of unimodal distributions with sample size n to have a specific Dip value d or more. Based on the desired Dip value d , the probability P will differ. So, as the final result of this, we get a table of different Dip values d for different sample sizes n . Each of those Dip values can then be assigned to a probability P of a unimodal function of the same sample size to have a Dip of d or greater. An example of such a table can be found in Hartigan and Hartigan (1985) Table 1. The only difference is that they calculated the probabilities for the Dip to be d or less (instead of d or greater). So a P-value of 1 means, that the distribution is unimodal with a 100% probability while a P-value of 0 indicates a totally multimodal distribution.

We can now compare the Dip of our empirical data distribution to this table and make conclusions. The original table of Hartigan and Hartigan (1985) states that a unimodal distribution of sample size 100 has a 90% probability to have a Dip of 0.0274 or more. Let's assume that we calculated the Dip for our dataset to be exactly 0.0274. By comparison we can say, that our dataset is presumably unimodal, at least with a 90% probability. The table from the original paper also states, that only 0.1% of unimodal distributions with sample size 100 have a Dip of 0.0687 or more. So if the dip of our empirical dataset is for example 0.07, we can say with good confidence that it is at least bimodal.

3 Results

3.1 The original Mt. Wilson dataset (Noyes et al. 1984)

The diptest was performed on the data used by Noyes et al. (1984) to test its bimodality. The Dip is calculated to be 0.04496, which doesn't say anything on its own and has to be considered in regard to the sample size n , which is 84 data points between $0.44 < B-V < 1.1$. With this n we can calculate a P-value of 0.24007. This means, that this distribution of data points is unimodal only with a 24% probability. Thus, there is a chance of 76% for it to have more than one mode, thus being bi-/multimodal. Consequently, the gap appears to be evident in this dataset.

Fig. 8 shows the cumulative distribution function of the data used by Noyes et al. (1984) in red as well as the best fitting unimodal distribution in blue. The two black lines are the cumulative distribution function shifted up/down by the Dip value for better visualization. This shift seems to be rather big in comparison with the overall sample size, which indicates bimodality. This is, as mentioned earlier, also supported by the Dip and the P-value.

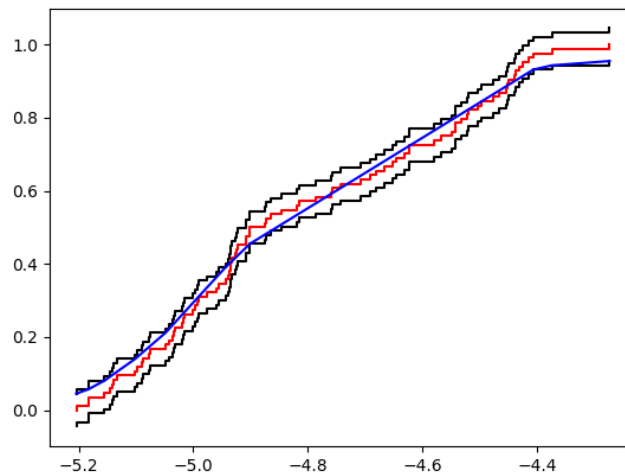


Figure 8: Cumulative distribution function (red) of the data from Noyes et al. (1984) (histogram can be seen in Fig. 5). The x-axis represents the R'_{HK} while the y-axis stands for the probability and goes from 0 to 1. The blue line is the best fitting unimodal distribution. The maximum difference between this blue line and the cumulative distribution function is the Dip. The upper/lower black line is the original cumulative distribution function shifted by the Dip value to the top/bottom.

3.2 The new dataset

Fig. 9 shows the histogram of the whole dataset. As expected by looking at Fig. 6, it does not seem unimodal. There can be probable peaks identified at around -4.0, -4.5 and -5.0. When running the Diptest with this sample, the results back up these findings. The Dip is 0.01 with a rounded P-value of 0.04. This means that only 4% of all unimodal distributions with the same sample size have a Dip which is equal or bigger than 0.01. Thus, there is a 96% probability of this dataset to have more than one mode. This stems from the fact that for example between $1.1 < B-V < 1.4$ there seems to be this slope of activity levels for all stars. In other words, F- and G-stars can be less active than K-stars. When going to B-V greater than 1.4, there is also a greater scatter of activity levels again. This arises from the fact that in this range the stars are mostly faint M-dwarfs. It is fairly difficult to measure the B-V and the $\log R'_{HK}$ of these stars with reasonably good accuracy. The diptest was also performed on the entire sample. Fig. 10 shows the cumulative distribution function of the new dataset. Due to the big sample size, the Dip is not visible at all and thus there are no additional insights to be gained from these plots for the following datasets. This said, those plots are not included in this

work. Only the important numbers such as the Dip and the P-value are noted for each subset, for these are sufficient to decide, whether a distribution is uni- or bimodal.

Because the whole dataset is clearly not unimodal and there is no physical incentive to try to investigate that any further, the dataset was split up into three different subsets. The first one consists of 2322 mostly F- and G-stars from $0.44 < B-V < 1.1$. This is also the most interesting dataset because the VP-Gap is defined on this interval and to check the existence of this gap is the aim of this investigation. The next set contains 290 stars with $1.1 < B-V < 1.4$, which are basically the K-stars. This has to be a separate subset because there is this prominent slope present, which was already mentioned earlier. If those stars would be included in a bigger B-V range, this would distort the distribution of the whole set. And lastly, M-stars from $1.4 < B-V < 2.0$ define another subset. This is the smallest dataset with 223 stars and features the biggest scatter of the three.

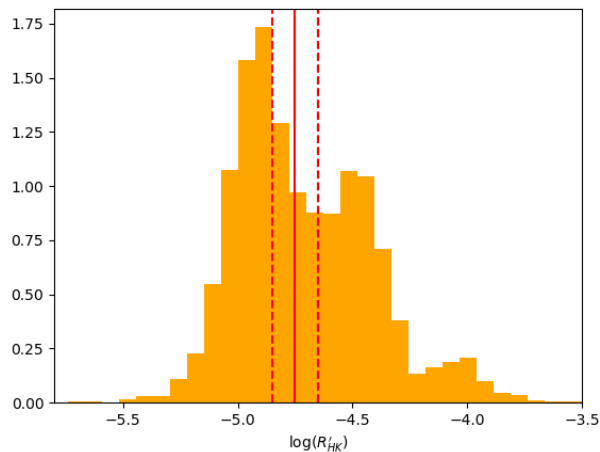


Figure 9: Histogram of all the data from Fig. 6. The red lines indicate the VP-Gap. This dataset as a whole is not unimodal because it contains different spectral types with different physical mechanisms.

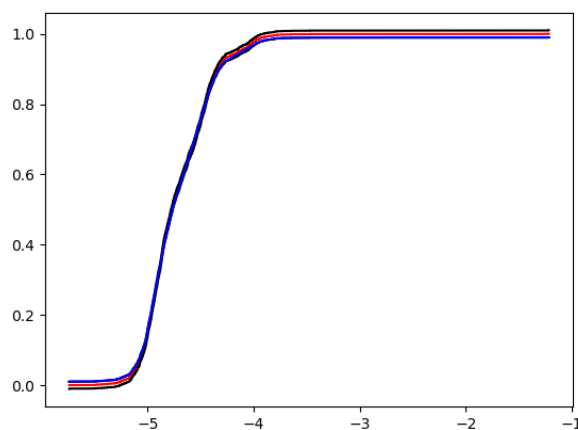


Figure 10: Cumulative distribution function and the fitted unimodal distribution as well as the gap just like in Fig. 8. Due to the very big sample size, neither the Dip nor the fitted function is visible, thus the plots for the subsequent subsets of this data will not be included in this work.

3.3 The three subsets

3.3.1 Subset 1: $0.44 < B-V < 1.1$

The first dataset examined contains stars with $0.44 < B-V < 1.1$. Thus, the majority of these stars are either F- or G-stars. This is the exact interval of B-V as Vaughan and Preston (1980) and Noyes et al. (1984) investigated. For that reason, the VP-Gap is only defined on this section and should be visible somewhere between $-4.85 < \log R'_{HK} < -4.65$. The histogram alone, shown in Fig. 11, makes it rather clear, that the VP-Gap is almost non-existent, at least not between the original boundaries (dotted red lines). Furthermore, it appears, that this distribution is represented in the histogram of the whole dataset (Fig. 9) as the leftmost peak at around $\log R'_{HK} = -5.0$.

After running the Diptest on this sample, a Dip of 0.00613 is obtained. Together with the sample size of 2322 stars, it also provides a P-value of 0.87793, meaning that with almost an 88% probability, this subset of stars is distributed in a unimodal way. Therefore, there is only a 12% chance that these stars exhibit two or more separate peaks (bi-/multimodal). We therefore can conclude, that this distribution is most likely unimodal. If it is indeed unimodal, this would mean, that the VP-Gap is definitely not present in this dataset.

Additionally, a normal distribution was fitted to this subset, resulting in the black line in Fig. 11. If the sample would show a normal distribution, according to the fit, its center would be at $\mu = -4.75808$ with a standard deviation of $\sigma = 0.26669$. As can be easily spotted in the plot below, the fitted curve does not align very well with the histogram. This is also expressed by the small coefficient of determination of $R^2 = 0.16353$. This parameter ranges from 0 to 1 and if the fit would have been perfect, this should be 1. Although the fit of the normal distribution does not describe the real distribution, this says nothing about unimodality. The sample can still be unimodal, only with an overlap of different unimodal distributions to form again a unimodal distribution. A case, where this can happen is illustrated in Fig. 7(a).

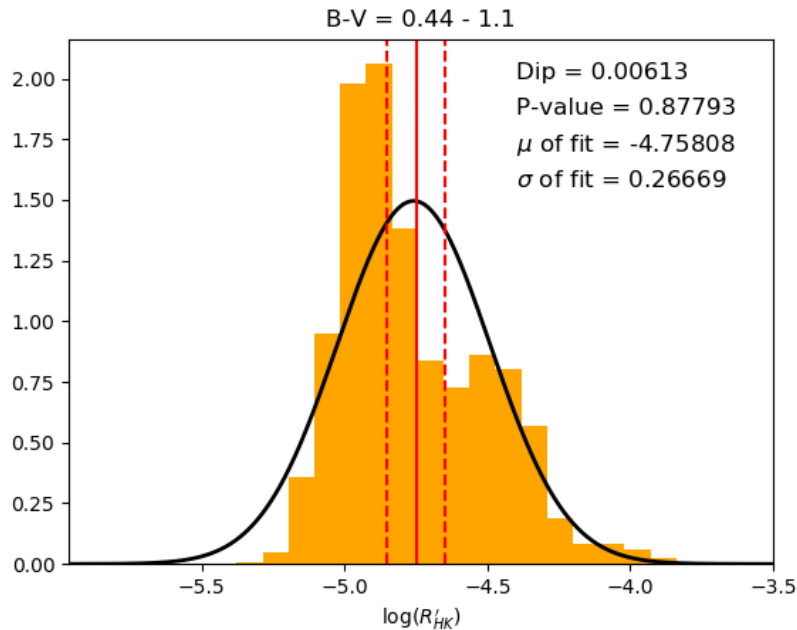


Figure 11: Histogram of subset 1. It shows the distribution of 2322 F- and G-stars. Vaughan and Preston (1980) looked at the same spectral types, thus the VP-Gap is defined on this range of B-V. The dotted red lines indicate the area, where the gap should be. Unlike with the samples from the 1980s, the gap is not visible with the bare eye. According to the Diptest, the distribution should be unimodal with a 87.8% probability. The solid black line is a fitted normal distribution to the data with $R^2 = 0.16353$.

3.3.2 Subset 2: $1.1 < B-V < 1.4$

The next subset to investigate consists of 290 K-stars with $1.1 < B-V < 1.4$. This sample is by far smaller than subset 1, for we only got around 10% of the stars, and it is also the area of the activity slope in Fig. 6. By looking at the histogram alone, it also seems that it is distributed in a unimodal fashion as well. The VP-Gap is again indicated by the dotted red lines in Fig. 12, but it does not occur to be an actual feature of the data sample. In Fig. 9, these stars probably produce the middle peak at around $\log R'_{HK} = -4.5$.

The Diptest resulted in a Dip of 0.01459 and a P-value of 0.97505. This lets us draw the conclusion, that with almost 100% certainty, this dataset is distributed unimodally and only 2.5% of all simulated unimodal distributions with $n = 290$ had a Dip even smaller than 0.01459. Thus, we conclude, that this dataset is probably unimodal.

Again, a normal distribution was fitted to the data, this time describing the distribution better than it did for subset 1. Its mean value, its peak, is at $\mu = -4.55874$. The standard deviation is $\sigma = 0.24067$. This fits the peak of the histogram pretty well, which is also reflected in the coefficient of determination $R^2 = 0.37986$, although it is by far not perfect. This imperfection likely arises from the fact that the underlying distribution function of the dataset is a different one.

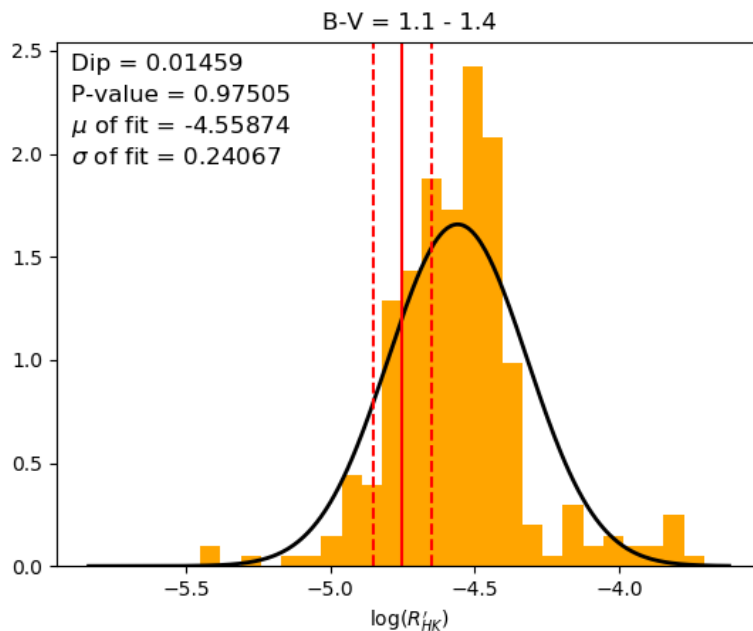


Figure 12: Histogram of subset 2, containing 290 K-stars. The dotted red lines show again the area of the VP-Gap, although it was not defined on this B-V range in the first place. With a 97.5% probability, we can say, that this is a unimodal distribution. The solid black line is again the fitted normal distribution to the dataset with $R^2 = 0.37986$.

3.3.3 Subset 3: $1.4 < B-V < 2.0$

The last set of stars contains M-stars from $1.4 < B-V < 2.0$. The histogram looks bimodal with peaks at around -5.1 and -4.5, with the VP-Gap fitting pretty well in between, although it was not originally defined on this B-V range. Presumably it can be explained by the fact, that in this area, the scatter of activity levels is rather big compared to the previous two subsets. This stems from the types of stars within the set, which is mostly very faint M-dwarfs. Due to the small luminosity from these objects, it is very hard to precisely measure B-V and R'_{HK} , which in return can result in this kind of scatter. Furthermore, the sample size of 223 is also not big enough to be able to compensate for this measurement error.

The results of the Diptest provide a Dip of 0.02558 and corresponding P-value of 0.40374. Consequently, the distribution is unimodal with a 40% chance and bi- or multimodal with a 60% chance. Thus, no reliable statements can be made. The accuracy of the Diptest and consequently the reliability of the P-value can be vastly increased with bigger sample sizes, so the M-dwarfs form a sample which is predestined for further investigation in the future when we will have obtained even more data.

The fit of the normal distribution is again not very good. It does not seem to resemble the real distribution of the data. This time, it can be the result of the whole distribution not being unimodal in the first place. Nonetheless, having a $R^2 = 0.22496$, it appears to fit better to the data than it did for the first subset. Its center is at $\mu = -4.83866$ with a standard deviation of $\sigma = 0.34738$.

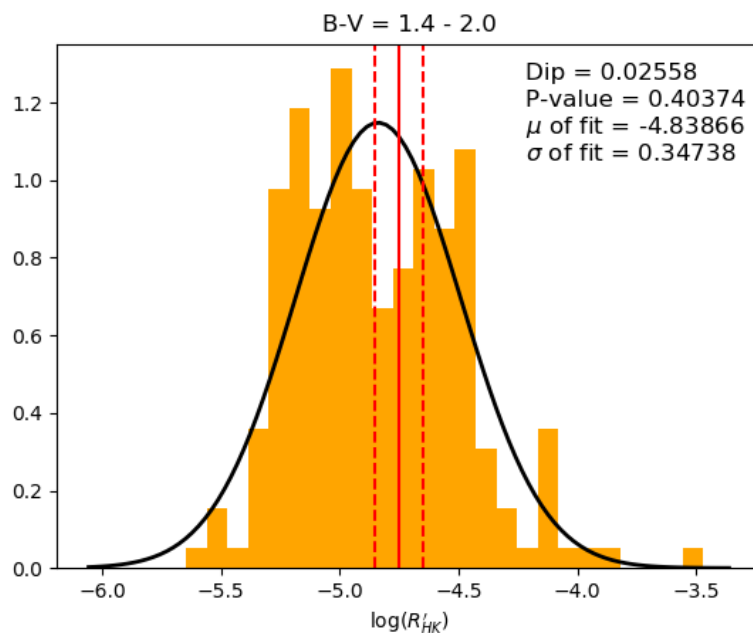


Figure 13: Histogram of subset 3. It contains 223 M-stars in the range $1.4 < B-V < 2.0$. The VP-Gap (dotted red line) seems to fit better to the distribution, leading to the belief that it is bimodal. The Diptest does not help us in making any conclusions about the dataset. According to the test, it could be either uni- or bimodal with almost the same probability. The fitted normal distribution (solid black line) has a coefficient of determination of $R^2 = 0.22496$.

3.4 Observational evidence of the nonexistence of the VP-Gap

Chromospheric activity is a manifestation of the stellar magnetic fields, which in turn depend on stellar rotation. The different levels of activity suggest that the rotation rate is different for these stars. One of the possible explanations of the existence of the VP-Gap is the non-existence of mid-activity stars, implying the non-existence of mid-rotating stars. Hence, the relation between activity, rotation and B-V in the current sample can provide valuable information. So, in addition to determining the statistical significance of the VP-Gap in the sample, the rotational velocity of the stars was obtained from Simbad³ and compared to their activity data.

Since it is not possible to measure the real rotation velocity of stars, but only the projected radial velocity via line broadening in the spectrum of a star, $vsini$ is used instead. v is the actual rotation velocity of the star and i is the inclination under which we observe the star. Therefore, we can never measure a greater rotation velocity but almost always measure a velocity smaller than v (for $i \neq 0$). Despite the uncertainty of rotation velocity, it is possible to draw statistical conclusions from it if our sample is big enough. This is possible if we make the assumption that the rotation axis of stars, on which the inclination i depends on, is distributed uniformly in space. Thus, we can say that the mean value of $sini$ should be $\pi/4$.

The rotation rate, $vsini$, was collected for 1198 out of our sample of 3064 stars. 905 of those are in the range $0.44 < B-V < 1.1$ and have a $vsini > 5$ km/s. The constraint on rotation rate has to be made because with such small $vsini$, the uncertainty of the measurement is usually bigger than the actual velocity.

This sample is now significantly smaller than the sample from section 3.3.1, which causes the VP-Gap to be visible again. That should be, like Vaughan and Preston (1980) and Noyes et al. (1984) also experienced, just a statistical sampling effect. As a validation of the gap being present, the Dip test was done on this reduced sample as well, resulting in a Dip of 0.02556 and a P-value of 0.00033. This indicates to the dataset being almost certainly bi-/multimodal. Also the fit of the normal distribution to the data with a mean value of $\mu = -4.67704$ and a standard deviation of $\sigma = 0.27518$ does not describe the real distribution of the data at all. Not surprisingly, the coefficient of determination is also very low at $R^2 = 0.05211$.

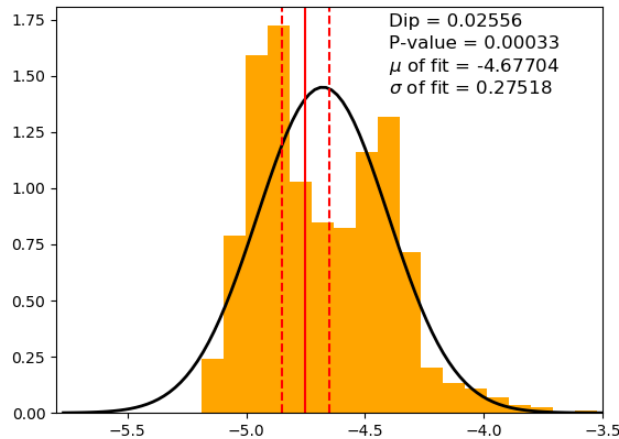


Figure 14: Histogram and Dip statistics of the reduced sample of 905 stars with $0.44 < B-V < 1.1$. It shows clear bimodality with a Dip of 0.02556 and a P-value of 0.00033. In the histogram alone, a gap in activity can be spotted with the bare eye. The VP-Gap is indicated by the dotted red lines, the normal fit to the data with $R^2 = 0.05211$ is visualized by the solid black line.

Having the data all together, chromospheric activity $\log R'_{\text{HK}}$ is plotted versus the rotation rate $\log vsini$. There is a huge spread in $vsini$, so the logarithm is used. As shown in Figures 15 and 16, there seems to be only a weak correlation between the chromospheric activity and the rotation rate. Nonetheless, there is an upwards trend visible of higher activity with higher rotation rate.

³<http://simbad.u-strasbg.fr/simbad/>

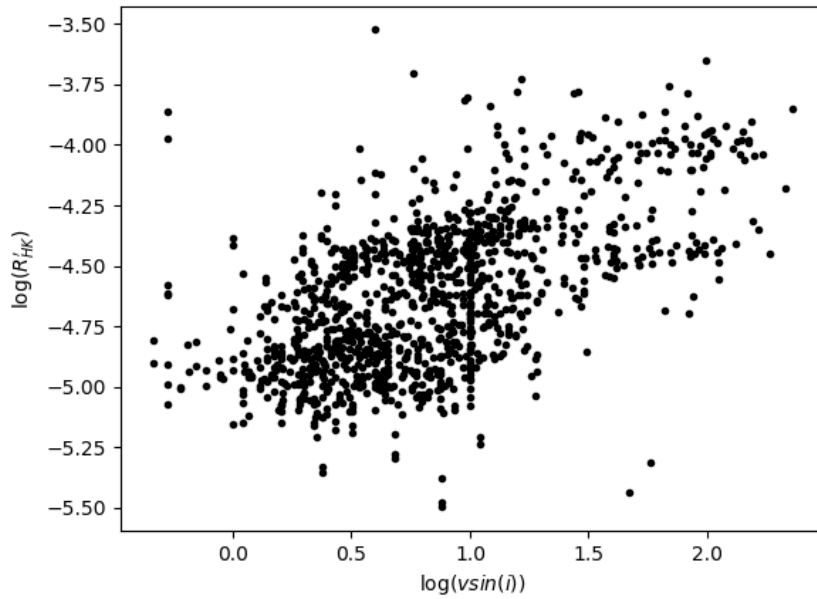


Figure 15: Plot of the chromospheric activity $\log R'_{HK}$ versus the projected rotation rate $\log v \sin i$ for the whole dataset consisting of 1198. There is an upwards trend visible.

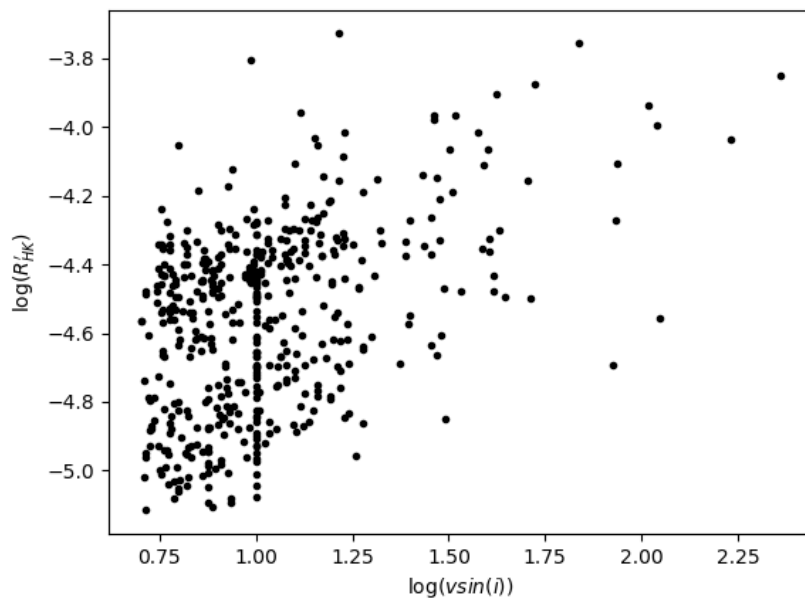


Figure 16: Plot of the chromospheric activity $\log R'_{HK}$ versus the projected rotation rate $\log v \sin i$ of stars between $0.44 < B-V < 1.1$ and $v \sin i > 5$ km/s. There is again an upwards trend visible that higher rotation rate means higher chromospheric activity.

To be able to better visualize these results, B-V is plotted against $\log R'_{\text{HK}}$ just like in Fig. 6 (this time with the reduced sample of 1198 stars) with rotation rate information added to it. This can be seen in Fig. 17. The coloring indicates the $\log v \sin i$. Again, the logarithm of the rotation rate is used for better visualization in the plot. Yellow means high rotation rate of up to 200 km/s, blue indicates low rotation rates with a lower boundary of 5 km/s.

There is again a clear trend to be seen of very active stars (mostly F-stars) with high rotation rate in the top left corner to more or less inactive stars with low rotation rate on the bottom of the plot. Additionally, it can be spotted that active K- and M-stars with $B-V > 1.1$ do not have to have a high rotation rate to show high activity. This can probably be attributed to the fact that these cool stars can have extended convective envelopes producing a strong magnetic field and thus heating the chromosphere. Additionally, the VP-Gap is apparent, which is due to the small sample size. However, one important point is that we do see some mid-activity stars and that these mid-activity stars are rotating with intermediate $v \sin i$. This shows, that intermediately rotating stars do exist but in order to detect them, a big enough sample is required.

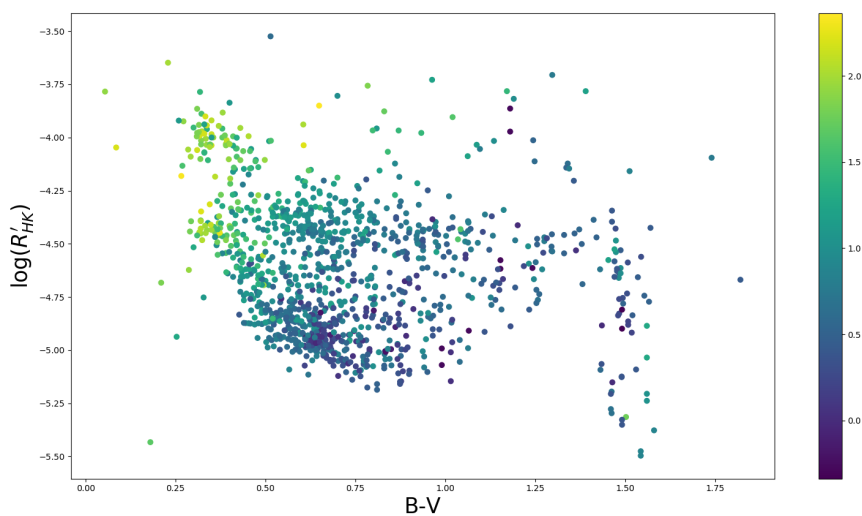


Figure 17: Color index B-V versus chromospheric activity $\log R'_{\text{HK}}$ with additional rotation rate information. There is a trend visible of fast rotating stars with high activity to slow rotating stars with little activity. An exception are cool stars like K- and M-stars with $B-V > 1.1$.

4 Discussion and Conclusion

3064 stars with $0.44 < B-V < 2.0$, thus ranging from F-stars to M-dwarfs, were analyzed in regard to the unimodality of the distribution function.

The whole dataset used in this work is not unimodal. This can be attributed to the different spectral classes, which can be found in this big sample. The stars range from F-stars to M-dwarfs. Because of that, these stars exhibit big differences in the height of their convective zones. Therefore, we expect them to have different magnetic properties and because chromospheric activity is dependent on the magnetic field generation, these stars cannot be grouped together into one general group.

The results of the Diptest for the F- and G-stars ($0.44 < B-V < 1.1$) clearly show the unimodality of this dataset with a probability of 87.8%. This is the exact B-V range, in which the VP-Gap is defined. Due to the unimodality of this vastly greater dataset compared to the one from Vaughan and Preston (1980) and Noyes et al. (1984), we can conclude, that there is no gap in activity. Hence, also stars with intermediate activity are found with the same chance as stars with high or low activity. Poor sampling effects could be blamed for the existence of the gap. This rules out the former explanation attempts of why the VP-Gap is present. The gap is neither a real feature of stars in the solar neighborhood, nor is it a feature of stars in general. Furthermore, if the gap does not exist in the first place, there is no need for such theories as a rapid spindown or different dynamo mechanisms. Preliminary indication of such smooth spindown is shown in Fig. 17. Therefore, stars spin down smoothly, as one would expect in the first place. They start as young stars with high rotation rate and high activity and evolve into slowly spinning stars with low activity. This transition does not happen fast but rather continuously. As mentioned earlier, if there are no two branches of activity levels, we can also rule out the presence of different dynamo mechanisms. Thus the magnetic fields are created/enhanced by the same physical mechanism and this should not change in a stars lifetime when it transitions from "young" to "old". The next sample of K-stars ($1.1 < B-V < 1.4$) shows even stronger unimodality. This is probably due to the slope in activity levels of these stars, which is why they are not as spread out as others.

The last sample consists of mostly faint M-dwarfs ($1.4 < B-V < 2.0$), which show neither strong uni- nor bimodality. The probability of the sample being unimodal is only 40%, which leaves a chance of 60% of it being bi-/multimodal. Due to this, we cannot draw any good conclusions in terms of their distribution. A possible explanation of why this dataset is not unimodal is, that as mentioned before, it consists of mainly faint stars, for which the chromospheric activity is hard to measure with high precision.

All in all, stars seem to be distributed in a unimodal fashion when it comes to chromospheric activity, thus there should not be any gaps in between.

List of Figures

1	Chromospheres photographed by Roberts (1945)	2
2	CAII H & K lines	3
3	$\log S$ vs. B-V, Vaughan and Preston (1980)	5
4	$\log R'_{\text{HK}}$ vs. B-V, Noyes et al. (1984)	6
5	Histogram of the data from Noyes et al. (1984)	7
6	B-V vs. R'_{HK} plot of the whole dataset	8
7	Distributions with different $\mu_1, \sigma_1, \mu_2, \sigma_2$ values. (a) $\mu_1 = 45, \sigma_1 = 10, \mu_2 = 55, \sigma_2 = 10$. (b) $\mu_1 = 40, \sigma_1 = 10, \mu_2 = 65, \sigma_2 = 10$. (c) $\mu_1 = 50, \sigma_1 = 4, \mu_2 = 60, \sigma_2 = 4$	9
8	Cumulative Distribution and Diptest with data from Noyes et al. (1984)	11
9	Histogram of the whole dataset	12
10	Cumulative Distribution and Diptest of the whole dataset	12
11	Diptest and normal fit of $0.44 < \text{B-V} < 1.1$	13
12	Diptest and normal fit of $1.1 < \text{B-V} < 1.4$	14
13	Diptest and normal fit of $1.4 < \text{B-V} < 2.0$	15
14	Diptest and normal fit of the whole dataset with rotation rate information	16
15	$\log R'_{\text{HK}}$ vs. $\log vsini$ of the whole dataset with rotation rate information	17
16	$\log R'_{\text{HK}}$ vs. $\log vsini$ of $0.44 < \text{B-V} < 1.1$	17
17	B-V vs. R'_{HK} of the whole dataset with rotation rate information	18

References

- [Arriagada (2011)] Arriagada, P., 2011, "Chromospheric Activity of Southern Stars from the Magellan Planet Search Program", *Astrophys. J.*, 734, 70
- [Baliunas and Soon (1995)] Baliunas, S.L., Soon, W.H., 1995, "Are Variations in the Length of the Activity Cycle Related to Changes in Brightness in Solar-Type Stars?", *Astrophys. J.*, 450, 896–901
- [Baliunas et al. (1995)] Baliunas, S.L., Donahue, R.A., Soon, W.H., Horne, J.H., Frazer, J., et al. , 1995, "Chromospheric variations in main-sequence stars", *Astrophys. J.*, 438, 269-287
- [Baliunas et al. (1998)] Baliunas, S.L., Donahue, R.A., Soon, W.H., Henry, G.W., 1998, "Activity Cycles in Lower Main Sequence and Post Main Sequence Stars: The HK Project", in *Cool Stars, Stellar Systems, and the Sun*, (Eds.) Donahue, R.A., Bookbinder, J.A., Proceedings of the Tenth Cambridge Workshop, held at Cambridge, Massachusetts, 15 – 19 July 1997, vol. 154 of ASP Conference Series, pp. 153–172, Astronomical Society of the Pacific, San Francisco
- [Biermann (1948)] Biermann, L., 1948, "On the Cause of Chromospheric Turbulence and UV Excess of Solar Radiation", *Z. Astrophys.*, 25, 161–177
- [Böhm-Vitense (2007)] Böhm-Vitense, E., 2007, "Chromospheric Activity in G and K Main-Sequence Stars, and What it Tells Us About Stellar Dynamos", *Astrophys. J.*, 657, 486–493
- [Bonfils et al. (2013)] Bonfils, X., Delfosse, X., Udry, S., Forveille, T., Mayor, M., et al. , 2013, "The HARPS search for southern extra-solar planets. XXXI. The M-dwarf sample", *A&A*, 549, 109
- [Boro Saikia et al. (2018)] Boro Saikia, S., Marvin, C.J., Jeffers, S.V., Reiners, A., Cameron, R., et al. , 2018, "Chromospheric activity catalogue of 4454 cool stars. Questioning the active branch of stellar activity cycles", eprint arXiv:1803.11123
- [Duncan et al. (1991)] Duncan, D.K., Vaughan, A.H., 1991, "CA II H and K Measurements made at Mount Wilson Observatory, 1966-1983", *Astrophys. J. Suppl. Ser.*, 76, 383-430
- [Durney et al. (1981)] Durney, B.R., Mihalas, D., Robinson, R.D., 1981, "A Preliminary Interpretation of Stellar Chromospheric Ca II Emission Variations Within the Framework of Stellar Dynamo Theory", *Publ. Astron. Soc. Pac.*, 93, 537–543
- [Eberhard & Schwarzschild (1913)] Eberhard, G., Schwarzschild, K., 1913, "On the reversal of the calcium lines H and K in stellar spectra", *Astrophys. J.*, 38, 292-295
- [Gray et al. (2006)] Gray, R.O., Corbally, C.J., Garrison, R.F., McFadden, M.T., Bubar, E.J., et al. , "Contributions to the nearby stars (nstars) project: spectroscopy of stars earlier than M0 within 40 pc - the southern sample", *The Astronomical Journal*, Volume 132, Issue 1, pp. 161-170
- [Hall et al. 2008] Hall, Jeffrey C., 2008, "Stellar Chromospheric Activity", *Living Rev. Solar Phys.*, 5, (2008), 2
- [Hall et al. (2009)] Hall, J. C., Henry, G. W., Lockwood, G. W., Skiff, B. A., Saar, S. H., 2009, "The activity and variability of the sun and sun-like stars. II. Contemporaneous photometry and spectroscopy of bright solar analogs", *The Astronomical Journal*, Volume 138, Issue 1, pp. 312-322
- [Hartigan and Hartigan (1985)] Hartigan, J.A., Hartigan, P.M., 1985, "The Dip Test of Unimodality", *The Annals of Statistics*, Vol. 13, No. 1, 70-84
- [Henry et al. (1996)] Henry, T. J., Soderblom, D. R., Donahue, R. A., Baliunas, S. L., 1996, "A Survey of Ca II H and K Chromospheric Emission in Southern Solar-Type Stars", *Astronomical Journal*, 111, 439
- [Isaacson & Fischer (2010)] Isaacson, H., Fischer, D., 2010, "Chromospheric Activity and Jitter Measurements for 2630 Stars on the California Planet Search", *The Astrophysical Journal*, Volume 725, Issue 1, pp. 875-885

- [Linsky (2017)] Linsky, J.L., 2017, "Stellar Model Chromospheres and Spectroscopic Diagnostics", Annual Review of Astronomy and Astrophysics, vol. 55, issue 1, pp. 159-211
- [Lovis et al. (2011)] Lovis, C., Dumusque, X., Santos, N. C., Bouchy, F., Mayor, M., et al. , 2011, "The HARPS search for southern extra-solar planets. XXXI. Magnetic activity cycles in solar-type stars: statistics and impact on precise radial velocities", eprint arXiv:1107.5325
- [Mamajek & Hillenbrand (2008)] Mamajek, E.E., Hillenbrand, L.A., 2008, "Improved Age Estimation for Solar-Type Dwarfs Using Activity-Rotation Diagnostics", The Astrophysical Journal, Volume 687, Issue 2, pp. 1264-1293
- [Middelkoop (1982)] Middelkoop, F., 1982, "Magnetic Structure in Cool Stars. IV. Rotation and Ca II H and K Emission of Main-sequence Stars", A&A, 107, 31
- [Mittag et al. (2013)] Mittag, M., Schmitt, J.H.M.M., Schröder, K.-P., 2013, "Ca II H+K fluxes from S-indices of large samples: a reliable and consistent conversion based on PHOENIX model atmospheres", A&A, 549, 117
- [Noyes et al. (1984)] Noyes, R.W., Hartmann, L.W., Baliunas, S.L., Duncan, D.K., Vaughan, A.H., 1984, "Rotation, Convection, and Magnetic Activity in Lower Main-Sequence Stars", Astrophys. J., 279, 763-777
- [Pearson (1894)] Pearson, K., 1894, "Contributions to the Mathematical Theory of Evolution", Philosophical Transactions of the Royal Society of London. A, Volume 185, pp. 71-110
- [Roberts (1945)] Roberts, W.O., 1945, "A Preliminary Report on Chromospheric Spicules of Extremely Short Lifetime", Astrophys. J., 101, 136-142
- [Rutten (1984)] Rutten, R. G. M., 1984, "Magnetic structure in cool stars. VII. Absolute surface flux in Ca II H and K line cores", A&A, 130, 353
- [Schwarzschild (1948)] Schwarzschild, M., 1948, "On Noise Arising from the Solar Granulation", Astrophys. J., 107, 1-5.
- [Vaughan and Preston (1980)] Vaughan, A.H., Preston, G.W., 1980, "A Survey of Chromospheric Ca II H and K Emission in Field Stars of the Solar Neighborhood", Publ. Astron. Soc. Pac., 92, 385-391
- [White and Livingston (1981)] White, O. R., Livingston, W. C., 1981, "Solar luminosity variation. III - Calcium K variation from solar minimum to maximum in cycle 21", Astrophys. J., 249, 798-816
- [Wilson (1978)] Wilson, O.C., 1978, "Chromospheric Variations in Main-Sequence Stars", Astrophys. J., 226, 379-396
- [Wright et al. (2004)] Wright, J. T., Marcy, G. W., Butler, R. P., Vogt, S. S., 2004, "Chromospheric Ca II Emission in Nearby F,G,K, and M Stars", Astrophys. J., Volume 152, Issue 2, pp. 261-295
- [Zhao et al. (2013)] Zhao, J.K., Oswalt, T.D., Zhao, G., Lu, Q.H., Luo, A.L., Zhang, L.Y., 2013, "Tracers of Chromospheric Structure. I. CaII H&K Emission Distribution of 13000 F, G and K stars in SDSS DR7 Spectroscopic Sample", The Astronomical Journal, Volume 145, Issue 5, article id. 140, 9 pp.